

Two Types of Pyridine Ligands in Mononuclear and Dinuclear Copper(II) Carboxylates

Bojan Kozlevčar,* Anica Murn, Katja Podlipnik, Nina Lah, Ivan Leban, and Primož Šegedin

Faculty of Chemistry and Chemical Technology, University of Ljubljana, Aškerčeva 5,
P. O. Box 537, SI-1001 Ljubljana, Slovenia

RECEIVED DECEMBER 2, 2003; REVISED MARCH 11, 2004; ACCEPTED MARCH 11, 2004

Copper(II) acetate $[\text{Cu}(\text{OOCCH}_3)_2(\text{L}1)_2]$ ($\text{L}1 = 2,6\text{-diaminopyridine}$) (**1**), $[\text{Cu}(\text{OOCCH}_3)_2(\text{L}2)_2]$ ($\text{L}2 = 2\text{-amino-6-methylpyridine}$) (**2**) and benzoate compounds $[\text{Cu}_2(\text{OOC}_6\text{H}_5)_4(\text{L}1)_2] \cdot 2\text{CH}_3\text{CN}$ (**3**), $[\text{Cu}_2(\text{OOC}_6\text{H}_5)_4(\text{L}1)_2]$ (**4**), $[\text{Cu}_2(\text{OOC}_6\text{H}_5)_4(\text{L}2)_2]$ (**5**), $[\text{Cu}(\text{OOC}_6\text{H}_5)_2(\text{L}2)_2]$ (**6**), were synthesized and characterized. X-ray structure analysis revealed monomeric structure in **1** and **6**. In **1**, *cis* arrangement of the ligands was found, and *trans* in **6**, in an elongated octahedral CuO_4N_2 chromophore. The basal plane in **1** and **6** is formed by one co-ordinated oxygen atom from both carboxylates (Cu-O 1.9560(12)–2.007(3) Å) and pyridine nitrogen atom from two pyridine ligands (Cu-N 2.013(3)–2.282(14) Å), forming a CuO_2N_2 plane, while the second carboxylate oxygen atoms are more distant (Cu-O 2.488(3)–2.7648(16) Å). The dinuclear *paddle-wheel* central core was found in **5** (Cu-O 1.942(6)–1.992(6) Å), with pyridine nitrogen atoms in the axial positions (Cu-N 2.283(7), 2.284(7) Å). All compounds were characterized by magnetic measurements, electronic and vibrational spectroscopy and tested for fungal growth retardation activity.

Key words
copper
 π -stacking
structure
spectroscopy
carboxylates
pyridine ligands

INTRODUCTION

Two main types of copper(II) carboxylates, mononuclear (distorted octahedral) and dinuclear (*paddle-wheel*), respectively, have been observed.^{1,2} The diversity of these coordination compounds largely depends on the carboxylate radical tail and even more on the additional ligand, both directing the path of the synthesis *via* their size, shape, substituents, *etc.* The stabilization of these compounds often takes place *via* non-covalent intra or intermolecular forces as hydrogen-bonding or π -stacking interactions.³ Very common additional ligands are based on the pyridine molecule, due to a strong nitrogen coordination site in the ring. The groups on positions 2 and 6 on pyridine ring are playing especially important role in

this type of complexes. Alkyl groups may sterically hinder also pyridine nitrogen coordination site, while amino groups may stabilize the compound with hydrogen bonds in the same coordination sphere or inter-molecular. Additionally, alkyl and amino groups are electron donating and as such disfavour π -stacking interactions.³ The aim of this work is to correlate different carboxylates and pyridine-based ligands in copper(II) complexes with the selected properties and structural parameters of the investigated compounds.

In this paper, synthesis, characterization and fungicidal activity of copper(II) acetates and benzoates with 2,6-diaminopyridine and 2-amino-6-methylpyridine are presented.

* Author to whom correspondence should be addressed. (E-mail: bojan.kozlevcar@uni-lj.si)

EXPERIMENTAL

Materials

Grey-black 2,6-diaminopyridine L1 (2.00 g) was recrystallized from 50.0 mL of chloroform. The mixture was heated up to the boiling temperature, filtered, and left at 253 K for three hours. Precipitated colourless crystals were filtered off and dried in a desiccator over KOH for a day (yield 40 %). $[\text{Cu}_2(\text{OOCCH}_3)_4(\text{C}_6\text{H}_5\text{COOH})_2]$ was prepared from hot aqueous solution of copper(II) sulphate, benzoic acid and sodium benzoate by precipitation method. The other starting substances and solvents were purchased from commercial sources and used without previous purification.

Synthesis

 $[\text{Cu}(\text{OOCCH}_3)_2(\text{L1})_2]$ (L1 = 2,6-diaminopyridine) (**1**)

2,6-Diaminopyridine (0.44 g) was dissolved in 10.0 mL of acetonitrile. Simultaneously, 0.40 g of $[\text{Cu}_2(\text{OOCCH}_3)_4(\text{H}_2\text{O})_2]$ was dissolved in 15.0 mL of acetonitrile, while heated and then added to the L1 solution. The obtained blue-green solution was cooled down and left for 24 hours at 279 K. Precipitated violet crystals were filtered off and dried over glass fryth and for a day in a desiccator (yield 70 %). λ_{max} / nm 340, 580; μ_{eff} / BM 1.84.

Anal. Calcd for $\text{C}_{14}\text{H}_{20}\text{CuN}_6\text{O}_4$ ($M_r = 399.90$): C 42.1, H 5.04, N 21.0, Cu 15.9 %; found: C 42.2, H 4.92, N 20.8, Cu 15.9 %.

 $[\text{Cu}(\text{OOCCH}_3)_2(\text{L2})_2]$ (L2 = 2-amino-6-methylpyridine) (**2**)

The procedure was similar as already described.⁴ $[\text{Cu}_2(\text{OOCCH}_3)_4(\text{H}_2\text{O})_2]$ (0.40 g) was dissolved in 22.0 mL of acetonitrile. The solution was added to the acetonitrile (4.0 mL) solution of L2 (0.65 g). After 24 hours at 279 K, violet crystals were filtered off and dried for 24 hours in a desiccator (yield 91 %). λ_{max} / nm 315, 400sh (sh = shoulder), 545, 690; μ_{eff} / BM 1.94.

Anal. Calcd for $\text{C}_{16}\text{H}_{22}\text{CuN}_4\text{O}_4$ ($M_r = 397.92$): C 48.3, H 5.57, N 14.1, Cu 16.0 %; found: C 48.5, H 5.36, N 14.2, Cu 15.9 %.

 $[\text{Cu}_2(\text{OOCCH}_3)_4(\text{L1})_2] \cdot 2\text{CH}_3\text{CN}$ (**3**)

The procedure was similar as already described.⁵ 0.43 g of $[\text{Cu}_2(\text{OOCCH}_3)_4(\text{C}_6\text{H}_5\text{COOH})_2]$ was dissolved in acetonitrile (10.0 mL) and added to acetonitrile solution (10.0 mL) of 2,6-diaminopyridine L1 (0.22 g). After 24 hours at 279 K, green needle-like crystals were filtered off and left for a day in a desiccator (yield 85 %). λ_{max} / nm 335, 400sh, 735; μ_{eff} / BM 1.43.

Anal. Calcd for $\text{C}_{42}\text{H}_{40}\text{Cu}_2\text{N}_8\text{O}_8$ ($M_r = 911.92$): C 55.3, H 4.43, N 12.3, Cu 14.0 %; found: C 55.4, H 4.41, N 12.2, Cu 13.8 %.

 $[\text{Cu}_2(\text{OOCCH}_3)_4(\text{L1})_2]$ (**4**)

0.22 g of 2,6-diaminopyridine L1 was dissolved in 2.0 mL of acetone. In the other flask, 0.43 g of $[\text{Cu}_2(\text{OOCCH}_3)_4(\text{C}_6\text{H}_5\text{COOH})_2]$ was dissolved in 9.0 mL of acetone while

heated, and then added to the L1 solution. Green solution was left at 279 K for 2 hours. The green needle-like crystals were filtered off (they dim on air – unstable) and left for a day in a desiccator (yield 55 %). λ_{max} / nm 330, 400sh, 730; μ_{eff} / BM 1.45.

Anal. Calcd for $\text{C}_{38}\text{H}_{34}\text{Cu}_2\text{N}_6\text{O}_8$ ($M_r = 829.81$): C 55.0, H 4.13, N 10.1, Cu 15.3 %; found: C 54.8, H 4.08, N 9.94, Cu 15.3 %.

 $[\text{Cu}_2(\text{OOCCH}_3)_4(\text{L2})_2]$ (**5**)

In 7.5 mL of acetonitrile, 0.34 g of $[\text{Cu}_2(\text{OOCCH}_3)_4(\text{C}_6\text{H}_5\text{COOH})_2]$ was dissolved, and added to the solution of 0.11 g of 2-amino-6-methylpyridine L2 in 0.5 mL of acetonitrile. The solution was left at 279 K for 24 hours. Dark green crystals were filtered off and then dried on fryth and for 24 hours in a desiccator (yield 44 %). λ_{max} / nm 315, 390sh, 735; μ_{eff} / BM 1.39.

Anal. Calcd for $\text{C}_{40}\text{H}_{36}\text{Cu}_2\text{N}_4\text{O}_8$ ($M_r = 827.84$): C 58.0, H 4.38, N 6.77, Cu 15.4 %; found: C 57.7, H 4.18, N 7.11, Cu 15.3 %.

 $[\text{Cu}(\text{OOCCH}_3)_2(\text{L2})_2]$ (**6**)

0.34 g of $[\text{Cu}_2(\text{OOCCH}_3)_4(\text{C}_6\text{H}_5\text{COOH})_2]$ was dissolved in 15 mL of acetonitrile, and added to the solution of 0.34 g of 2-amino-6-methylpyridine L2, dissolved in 3 mL of acetonitrile. Obtained blue-green solution was left at 279 K for 24 hours. In the first step, monomeric **6** and dimeric **5** benzoate compounds precipitated, however during next 24 hours, green crystals of **5** were dissolved and only dark violet crystals of **6** were filtered off. They were dried on glass fryth and 24 hours in a desiccator (yield 79 %). λ_{max} / nm 320, 405, 550, 705; μ_{eff} / BM 1.95.

Anal. Calcd for $\text{C}_{26}\text{H}_{26}\text{CuN}_4\text{O}_4$ ($M_r = 522.06$): C 59.8, H 5.02, N 10.7, Cu 12.2 %; found: C 59.7, H 4.86, N 10.9, Cu 12.5 %.

d-spacings (Å) and their relative intensities, from X-ray powder diffraction data for **1**, **2**, **4**, **3**, **5** and **6**, are in agreement with the calculated values^{6,7} from crystal structure analysis. X-ray powder diffraction pattern for **4** is completely reproducible for different samples (structure not solved).

X-ray Diffraction Work

Single crystal diffraction measurements were carried out on an Enraf-Nonius CAD4 diffractometer with graphite-monochromated Mo-K α radiation. Unit cell dimensions were obtained from 25 reflections in the θ range 8–16°. Common data corrections for variations in reference reflections and Lorentz polarization effects were applied.⁸ Absorption correction was performed by Gaussian integration method for **5** and **6**. No absorption correction was performed for compound **1**. Structures were solved by direct methods implemented in SHELXS-97 and refined by full matrix least squares on F^2 by SHELXL-97.⁹ Non-hydrogen atoms were refined anisotropically, hydrogen atoms were generated geometrically, assigned appropriate isotropic thermal displacement parameters and allowed to ride on their parent atoms.

Physical Measurements

Metal analysis was carried out electrogravimetrically with Pt electrodes. C,H,N analysis was performed with a Perkin Elmer, Elemental Analyzer 2400 CHN. Interplanar spacings were obtained by the Guinier camera (Huber and Enraf-Nonius) with Cu-K α radiation. The magnetic susceptibility of the substances was determined at room temperature by powdered samples with a Sherwood Scientific MSB-1 balance, using Hg[Co(NCS)₄] as a calibrant. Diamagnetic corrections were estimated from Pascal's constants.¹⁰ Infrared spectra were measured on mineral mulls between CsI plates, using a Perkin-Elmer FT-IR 1720X spectrometer. Electronic spectra were recorded as nujol mulls with a Perkin-Elmer UV/VIS/NIR spectrometer Lambda 19. Compounds were tested for fungicidal activity for wood decay fungi *Trametes versicolor* (L. ex Fr.) Pilat and *Antrodia vaillantii* (DC. ex Fr.) Ryv. as described previously.¹¹

RESULTS AND DISCUSSION

Description of the Crystal Structures

The coordination sphere in [Cu(OOCCH₃)₂(L1)₂] (L1 = 2,6-diaminopyridine) (**1**) is composed of two didentate acetate anions and two monodentate L1 molecules in *cis* conformation around the central copper(II) ion, forming

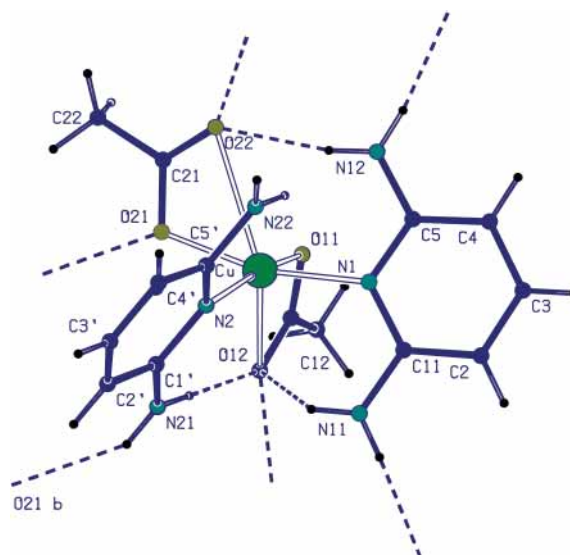


Figure 1. *Cis* arranged ligands in a distorted octahedral environment around copper ion in [Cu(OOCCH₃)₂(L1)₂] (**1**), with numerous H-bonds in 3D network.

a distorted octahedron (Figure 1). The crystallographic details are summarized in Table I. In the basal plane of the octahedron, one oxygen atom from both acetate groups is present (Cu–O11 2.007(3) Å, Cu–O21 1.971(3) Å) and the pyridine nitrogen atom from both pyridine-based lig-

TABLE I. Crystal data and data collection summary

	1	5	6
Formula	C ₁₄ H ₂₀ CuN ₆ O ₄	C ₄₀ H ₃₆ Cu ₂ N ₄ O ₈	C ₂₆ H ₂₆ CuN ₄ O ₄
<i>Mr</i>	399.90	827.84	522.06
Crystal system	orthorhombic	monoclinic	triclinic
Space group	<i>Pcab</i>	<i>P2₁/n</i>	<i>P</i> ₁
<i>a</i> / Å	14.357(3)	10.280(2)	7.5754(6)
<i>b</i> / Å	15.392(3)	20.930(10)	8.8374(9)
<i>c</i> / Å	15.448(3)	17.539(4)	10.5029(9)
α / °	90	90	74.495(8)
β / °	90	102.00(2)	71.942(8)
γ / °	90	90	77.820(10)
<i>V</i> / Å ³	3414(1)	3691(2)	637.84(10)
<i>Z</i>	8	4	1
<i>D_x</i> / g cm ⁻³	1.556	1.490	1.359
μ / mm ⁻¹	1.313	1.212	0.894
Crystal colour	violet	green	violet
Crystal shape	plate	prism	prism
Crystal size / mm	0.10 × 0.20 × 0.22	0.17 × 0.20 × 0.41	0.13 × 0.36 × 0.41
Intensity decay / %	2.8	2.1	1.1
Scan type	$\omega/2\theta$	$\omega/2\theta$	$\omega/2\theta$
θ range / °	2.35–27.98	1.95–26.50	2.09–27.95
Total data	15837	8034	6132
Independent data	4116	7605	3066
Observed data [<i>I</i> > 2 σ (<i>I</i>)]	1950	2854	2835
<i>R</i> ₁ (observed)	0.0509	0.0665	0.0346
<i>wR</i> ₂ (observed)	0.0890	0.1465	0.0910

ands (Cu–N2 2.013(3) Å, Cu–N1 2.025(3) Å). Significant difference is noticed in the distances of the remaining acetate oxygen atoms, that are semi-coordinated (Cu–O12 2.488(3) Å, Cu–O22 2.657(3) Å) on axial positions. The structure is stabilized by several hydrogen bonds among acetate oxygen atoms and amino groups from the pyridine ligands. The closer axial oxygen atom O12 participates in three H-bonds, intra-molecular to two pyridine ligands (N11–H···O12 3.119(5); N21–H···O12 2.893(5) Å) and one inter-molecular (N12–H···O12 2.900(4) Å). The semi-coordinated oxygen atom from the other acetate ion is forming one intra-molecular H-bond (N12–H···O22 2.910(5) Å) and one inter-molecular H-bond (N11–H···O22 3.035(4) Å). Only one oxygen atom in the first coordination sphere (Cu–O \approx 2.0 Å), participate in intra-molecular H-bond (N21–H···O21 3.040(4) Å). Interestingly three amino groups are included (Figure 1), each in two H-bonds, while for the fourth (N22) no such interactions were noticed. Extensive hydrogen-bonding network is obviously playing a key role in the asymmetric *cis* arrangement of the ligands in **1**.

The crystal structure analysis of $[\text{Cu}(\text{OOCCH}_2\text{C}_6\text{H}_5)_2(\text{L}2)_2]$ (**6**) revealed *trans* arrangement of benzoate anions and 2-amino-6-methylpyridine molecules L2 around the central copper(II) ion, lying on the inversion center. Like in **1**, one oxygen atom from both carboxylate anions (Cu–O 1.9580(12) Å) and pyridine nitrogen atom from 2-amino-6-methylpyridine molecules (Cu–N 2.028(14) Å) are composing the basal plane, while the remaining benzoate oxygen atoms from the two benzoates (Cu–O12 2.7648(16) Å) are occupying the axial positions. Similar geometry was observed in **2**.⁴ The amino group is forming an intra-molecular H-bond to the coordinated oxygen atom (N–H···O11 2.926(3) Å), and an inter-molecular H-bond to the semi-coordinated oxygen atom (N–H···O12 2.947(2) Å). Additional stabilization is found through π -stacking interactions between the aromatic rings of 2-amino-6-methylpyridine molecules (Figure 2) and also between benzoates; pyridine rings: $d(\text{c}_g\text{-c}_g)$ 3.9270(12) Å, α 0°, β 26.53°, benzene rings: $d(\text{c}_g\text{-c}_g)$ 3.9142(22) Å, α 0°, β 24.98°, c_g – centroid of the ring, α – angle between the planes of the rings, β – angle between $\text{c}_g\text{-c}_g$ vector and normal to plane of one ring.

The copper(II) ions in $[\text{Cu}_2(\text{OOCCH}_2\text{C}_6\text{H}_5)_4(\text{L}2)_2]$ (**5**), are bridged by four benzoate anions *via* carboxylate groups. The Cu–Cu distance of 2.7233(15) Å, is typical for the dinuclear *paddle wheel* type of copper coordination compounds.¹² The axial positions in the isolated dinuclear units are occupied by pyridine nitrogen atoms of 2-amino-6-methylpyridine molecules (Cu–N1 2.283(7), Cu–N2 2.284(8) Å). Each pyridine based ligand is forming an intra-molecular H-bond to one carboxylate oxygen atom (N11–H···O11 3.019(13) Å, N22–H···O32 3.133(12) Å). Both H-bonds in a dinuclear unit are *trans* oriented with respect to the center of the tetracarboxylate central core

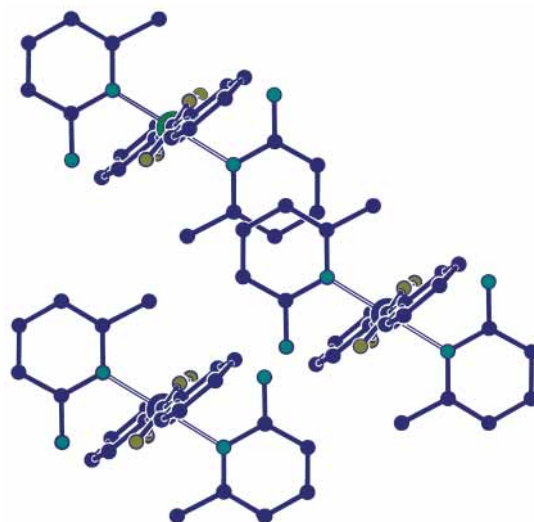


Figure 2. π -stacking interaction in $[\text{Cu}(\text{OOCCH}_2\text{C}_6\text{H}_5)_2(\text{L}2)_2]$ (**6**), among parallel pyridine rings in 2-amino-6-methylpyridine L2. All hydrogen atoms are omitted for clarity.

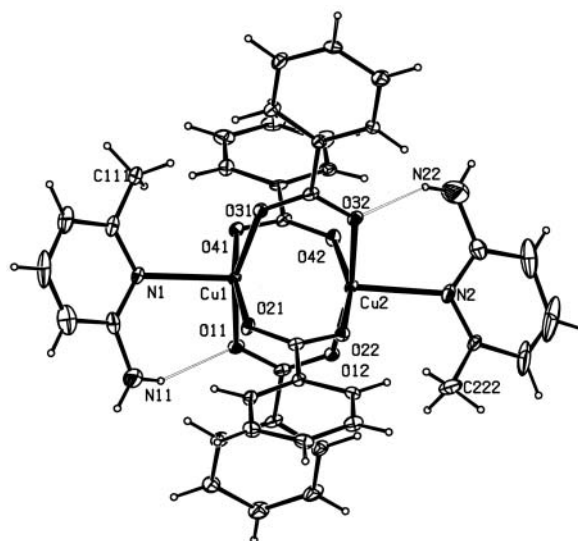


Figure 3. Intra-molecular hydrogen bonding in the dinuclear structure of $[\text{Cu}_2(\text{OOCCH}_2\text{C}_6\text{H}_5)_4(\text{L}2)_2]$ (**5**).

(Figure 3). Pyridine rings in the same dinuclear unit are almost co-planar (11(1)°). The pyridine rings are involved also in inter-dinuclear π -stacking interactions ($d(\text{c}_g\text{-c}_g)$ 3.7109(80) Å, α 0.03°, β 19.33°), which influence the crystal packing in the structure.

Magnetic Measurements and Spectroscopy

The results of magnetic measurements are in agreement with mononuclear ($\mu_{\text{eff}} > 1.73$ BM, for **1**, **2**,⁴ **6**) and dinuclear ($\mu_{\text{eff}} < 1.73$ BM, for **3**,⁵ **4**, **5**) nature of the compounds.

The electronic spectra of the dinuclear complexes **3–5** are similar, representing the bands of the d-d transition at 730 nm and LMCT at 400 nm and 320 nm, as observed in the spectrum of copper acetate hydrate.¹³ Nev-

TABLE II. IR (mineral oil mull) wave numbers/cm⁻¹

	$\nu(\text{NH}_2)_{\text{as}}$	$\nu(\text{NH}_2)_{\text{s}}$	$\delta(\text{NH}_2)$	$\nu(\text{C}-\text{C})_{\text{ar}}$	$\nu(\text{CO}_2)_{\text{as}}$	$\nu(\text{C}-\text{C})_{\text{ar}}, \nu(\text{CH}_3)_{\text{s}}$	$\nu(\text{CO}_2)_{\text{s}}$
1	3500–3150		1680–1620	1610–1600	1587, 1570–1540	1471	1439, 1401
2	3332	3191	1642, 1615	1580	1558	1476	1415
3	3500–3450	3400–3360	1645–1620	1598	1571	1470	1403
4	3497	3387	1640–1620	1599	1570	1463	1403
5	3492	3368	1640–1615	1610–1595	1574	1466	1404
6	3436, 3325, 3214		1632	1600	1560	1479, 1447	1386, 1374

ertheless, the UV region band partially originates also in π - π transitions, since it is observable in the spectra of pure ligands.

In the spectra of mononuclear compounds **2** and **6** (*trans* oriented ligands), two d-d transition bands were observed (~ 550 nm $d_{xz}, d_{yz} \rightarrow d_{x^2-y^2}$, ~ 700 nm $d_{xy} \rightarrow d_{x^2-y^2}$)^{13,14} and two LMCT transitions in the region towards higher energy (320, 400 nm).¹⁴ Such observations are in agreement with small rhombic deviations from axially elongated octahedral environment ($\text{Cu}-\text{O1} \ll \text{Cu}-\text{N} < \text{Cu}-\text{O2}$), found in **2** (Ref. 4) and **6**. On the other hand, only two bands (d-d at 580 nm, LMCT at 340 nm) were noticed in the spectrum of **1**, where *cis* arrangement of the ligands was found and less rhombic distortion of elongated axial octahedron ($\text{Cu}-\text{O1} \sim \text{Cu}-\text{N} \ll \text{Cu}-\text{O2}$). The presence of two signals instead of four is probably a consequence of smaller energy difference between orbitals from where the electron absorption to $d_{x^2-y^2}$ take place ($d_{yz}, d_{xz}, d_{yx}, d_{z^2}$ for d-d and ligand orbitals for LMCT transitions). In the other monomeric *cis* complex $[\text{Cu}(\text{OOCCH}_3)_2(2\text{-aminopyridine})_2]$ ¹⁵ also very small rhombic distortion was found, however the distance to axial semi-coordinated oxygen atoms do not differ so much as in **1**. In the spectrum of 2-aminopyridine complex, only one band was found in the 450–800 nm region as for **1**, while two bands in the lower energy region (310, 410sh) as in **2** and **6**.

NH_2 stretching vibrations in the IR spectra of dinuclear complexes **3–5** are noticed at 3500 cm⁻¹ (asymmetric $\nu(\text{NH}_2)_{\text{as}}$) and at 3380 cm⁻¹ (symmetric $\nu(\text{NH}_2)_{\text{s}}$), as found for their analogues with 2-aminopyridine.¹⁶ Both signals ($\nu(\text{NH}_2)_{\text{as}}, \nu(\text{NH}_2)_{\text{s}}$) split to three signals in the spectrum of solvated complex **3**. An analogy to 2-aminopyridine complexes was observed also for mononuclear compounds, where $\nu(\text{NH}_2)_{\text{as}}$ and $\nu(\text{NH}_2)_{\text{s}}$ are found at lower energies as for the dinuclear compounds. Additional band at 3436 cm⁻¹ for **6** and two in the same region for **1** are probably due to H-bonding network. In the region between 1800 and 1300 cm⁻¹ the bands for $\delta(\text{NH}_2)$, $\nu(\text{C}-\text{C})_{\text{ar}}$ (ar – aromatic) $\nu(\text{CO}_2)_{\text{as}}, \nu(\text{CH}_3)_{\text{s}}$ and $\nu(\text{CO}_2)_{\text{s}}$ are found (Table II).¹⁷ Splitting of the carboxylate group stretching bands for **1** is probably related to the nonequivalency of both carboxylate groups around the central copper ion. Similar splitting was noticed for not equivalent acetate groups in *cis* mononuclear 2-aminopyridine

complex.¹⁶ Lower energy of $\nu(\text{CO}_2)_{\text{s}}$ in benzoates than in related acetates is also an analogy to observed behavior in 2-aminopyridine complexes.¹⁶

The Influence of the Compounds on Fungal Growth

The tests on fungal growth for the species *Trametes versicolor* showed stronger activity for benzoate compounds than for acetates at concentration 1.0×10^{-3} mol L⁻¹, as already observed.^{11,18} Stronger retardation for benzoates was noticed also for *Antrodia vaillantii*, already at lower concentration 5.0×10^{-4} mol L⁻¹. No significant difference among mononuclear **6** and dinuclear **3–5** benzoates was noticed, therefore the results are not in agreement with predicted stronger fungicidal activity of the dinuclear complexes over mononuclear compounds.¹⁹ Nevertheless, we should not neglect the possibility, that the structures of solid compounds may change by dissolving in DMSO for the activity tests.

CONCLUSIONS

Monomeric complexes **1** and **2** (Ref. 4) differ in *cis* and *trans* arrangement of the ligands. In the structural database CSD, another two monomeric acetate complexes $[\text{Cu}(\text{OOCCH}_3)_2(\text{L})_2]$ with similar ligands 2-aminopyridine L3 (Ref. 15) and 2,6-dimethylpyridine L4 (Ref. 20) were found. The L3 complex is *cis* type as in **1**, while L4 complex is *trans* type, as found in **2**. In the cases of 2,6-dimethylpyridine and 2-methyl-6-aminopyridine, *trans* orientation is more stable, possibly due to less steric hindrance of methyl groups in *trans* than in *cis* conformation. On the other hand, in 2-aminopyridine and 2,6-diaminopyridine, amino groups enable strong hydrogen-bonding network that favourize *cis* orientation with respect to *trans*. Interestingly, in the acetate family with these four ligands $[\text{Cu}(\text{OOCCH}_3)_2(\text{L})_2]$ (L = L1, L2, L3, L4), only one dinuclear species $[\text{Cu}_2(\text{OOCCH}_3)_4(\text{L})_2]$ with L = L3, 2-aminopyridine, was found.¹⁶

For all four acetate mononuclear complexes (with L1, L2, L3 and L4) no π -stacking interactions were found, however two types (pyridine-pyridine and benzene-benzene) were noticed in the monomeric *trans* benzoate complex $[\text{Cu}(\text{OOCCH}_3)_2(\text{L}_2)_2]$ (**6**). All the other obtained benzoate complexes with 2-amino-6-methylpyridine and 2,6-diaminopyridine **3–5**, show the dinuclear struc-

ture, a significant difference from acetates with the same pyridine-based ligands (**1**, **2**).

The comparison of the investigated complexes **1–6**, show differentiation of acetates and benzoates in appearance of the mononuclear or the dinuclear complex structures. The reason for one mononuclear benzoate **6** (the others **3–5**) are dinuclear) might be in π -stacking interactions, observed in **6** but not in the acetate mononuclear compounds **1** and **2**. The leading role of the methyl and amino groups in pyridine-based ligands, was observed in monomeric complexes **1**, **2** and **6**, where their presence or absence seems to direct the path of the ligand arrangement around the central copper(II) ion in the octahedral coordination sphere.

Supplementary Materials. – CCDC– 222673 (**1**), 222674 (**5**), and 222672 (**6**) contain the supplementary crystallographic data for this paper. These data can be obtained free of charge at www.ccdc.cam.ac.uk/conts/retrieving.html on quoting the deposition numbers [or from the Cambridge Crystallographic Data Centre, 12, Union Road, Cambridge CB2 1EZ, UK; fax: (internat.) +44-1223/336-033; E-mail: deposit@ccdc.cam.ac.uk].

Acknowledgements. – The financial support of the Ministry of Education, Science and Sport, Republic of Slovenia, through grant PS-511-103 is gratefully acknowledged. We thank Prof. F. Pohleven from the Department of Wood Science and Technology, Biotechnical Faculty, University of Ljubljana, for fungal activity tests and Dr. S. Škapin from Ceramics Department, »Jožef Stefan« Institute, Ljubljana, Slovenia, for X-ray powder diffraction data.

REFERENCES

1. F. H. Allen, *Acta Crystallogr., Sect. B* **58** (2002) 380–388.
2. N. N. Greenwood and A. Earnshaw, *Chemistry of the Elements, second edition*, Butterworth-Heinemann, Oxford, 1997, pp. 1190–1193.
3. C. Janiak, *J. Chem. Soc., Dalton Trans.* (2000) 3885–3896.
4. N. Lah, L. Golič, P. Šegedin, and I. Leban, *Acta Crystallogr., Sect. C* **55** (1999) 1056–1058.
5. N. Lah, G. Giester, P. Šegedin, A. Murn, K. Podlipnik, and I. Leban, *Acta Crystallogr., Sect. C* **57** (2001) 546–548.
6. A. L. Spek, PLATON, University of Utrecht, The Netherlands, 2001.
7. L. J. Farrugia, *J. Appl. Cryst.* **30** (1997) 565.
8. E. J. Gabe, Y. Le Page, J.-P. Charland, F. L. Lee, and J. White, *J. Appl. Cryst.* **22** (1989) 384–387.
9. G. M. Sheldrick, SHELXS-97 and SHELXL-97, University of Goettingen, Germany, 1997.
10. R. L. Dutta and A. Syamal, *Elements of Magnetochemistry, second edition*, Affiliated East-West PVT Ltd., New Delhi, 1993, pp. 6–11.
11. T. Bergant, M. Petrič, F. Pohleven, J. Reberšek, and P. Šegedin, *Acta Chim. Slov.* **41** (1994) 393–404.
12. M. R. Sundberg, R. Ugglja, and M. Melnik, *Polyhedron* **15** (1996) 1157–1163.
13. B. J. Hathaway and D. E. Billing, *Coord. Chem. Rev.* **5** (1970) 143–207.
14. A. B. P. Lever, *Inorganic Electronic Spectroscopy, second edition*, Elsevier, Amsterdam, 1984, pp. 355–356, 557.
15. R. Grobelny, T. Glowiak, J. Mrozinski, L. Brzozka, W. Baran, and P. Tomasik, *Polish J. Chem.* **69** (1995) 559–565.
16. B. Kozlevčar, N. Lah, D. Žlindra, I. Leban, and P. Šegedin, *Acta Chim. Slov.* **48** (2001) 363–374.
17. G. Socrates, *Infrared Characteristic Group Frequencies, Tables and Charts, second edition*, John Wiley & Sons, Chichester, 1998.
18. B. Kozlevčar, I. Leban, I. Turel, P. Šegedin, M. Petrič, F. Pohleven, A. J. P. White, D. J. Williams, and J. Sieler, *Polyhedron* **18** (1999) 755–762.
19. M. Petrič, F. Pohleven, I. Turel, P. Šegedin, A. J. P. White, and D. J. Williams, *Polyhedron* **17** (1998) 255–260.
20. M.-M. Borel, A. Busnot, F. Busnot, A. Leclaire, and M.-A. Bernard, *Rev. Chim. Minerale*, **18** (1981) 370–375.

SAŽETAK

Dva tipa piridinskih liganada u mononuklearnim i dinuklearnim kompleksima Cu(II) karboksilata

Bojan Kozlevčar, Anica Murn, Katja Podlipnik, Nina Lah, Ivan Leban i Primož Šegedin

Pripravljene su i karakterizirani bakar(II) acetati $[\text{Cu}(\text{OOCCH}_3)_2(\text{L}1)_2]$ ($\text{L}1 = 2,6\text{-diaminopiridin}$) (**1**), $[\text{Cu}(\text{OOCCH}_3)_2(\text{L}2)_2]$ ($\text{L}2 = 2\text{-amino-6-metilpiridin}$) (**2**) te benzoati $[\text{Cu}_2(\text{OOC}_6\text{H}_5)_4(\text{L}1)_2] \cdot 2\text{CH}_3\text{CN}$ (**3**), $[\text{Cu}_2(\text{OOC}_6\text{H}_5)_4(\text{L}1)_2]$ (**4**), $[\text{Cu}_2(\text{OOC}_6\text{H}_5)_4(\text{L}2)_2]$ (**5**), $[\text{Cu}(\text{OOC}_6\text{H}_5)_2(\text{L}2)_2]$ (**6**). Rentgenska je strukturna analiza pokazala monomere u **1** i **6**. Izduženi oktaedarski CuO_4N_2 kromofor u **1** ima *cis*-, a u **6** *trans*-smještene ligande. Glavnu ravninu u **1** i **6** čine po jedan kisikov atom iz obje karboksilatne skupine $[\text{Cu}-\text{O} 1,9560(12)-2,007(3) \text{ \AA}]$ i dušikovi atomi dvaju piridinskih liganada $[\text{Cu}-\text{N} 2,013(3)-2,282(14) \text{ \AA}]$ tvoreći CuO_2N_2 ravninu, dok drugi kisikov atom karboksilatne skupine čini dulju vezu $[\text{Cu}-\text{O} 2,488(3)-2,7648(16) \text{ \AA}]$. Dinuklearna centralna jedinica konfiguracije mlinskoga kola nađena je u **5** $[\text{Cu}-\text{O} 1,942(6)-1,992(6) \text{ \AA}]$ s dušikovim atomima piridina u aksijalnim položajima $[\text{Cu}-\text{N} 2,283(7), 2,284(7) \text{ \AA}]$. Svi spojevi su karakterizirani magnetskim mjerjenjima, elektronskom i vibracijskom spektroskopijom i provjereni na antifungalno djelovanje.